Geotechnical Aspects of Underground Construction in Soft Ground – Yoo, Park, Kim & Ban (Eds)

E-Defense shaking test on large model of underground shaft and tunnels

I. Towhata
University of Tokyo, Tokyo, Japan

Y. Kawamata
National Research Institute for Earth Science and Disaster Prevention, Miki, Japan

M. Nakayama
Kobe Gakuin University, Kobe, Japan

S. Yasuda
Tokyo Denki University, Hiki, Japan

ABSTRACT: To obtain useful knowledge on detailed behaviors of underground structures and soil-structure interaction, shaking table testing method with large structure models is one of the most powerful options. The advantages of large-scale shaking table tests are; 1) large-scale models can minimize scale effects on soil and structure behavior, 2) image analysis technology that has developed in the recent times is applicable because significant displacement or deformation are generated in large structure models, and 3) a large number of various sensors can be placed where localized phenomenon are expected. In this paper, one of the world largest shaking tables, E-Defense, National Research Institute for Earth Science and Disaster Prevention, Japan, is introduced. In addition, the latest test series on interaction between soil and underground shaft and tunnels is described as an example of E-Defense tests.

1 INTRODUCTION

In urban areas, a large number of underground structures have been built mainly because of the limited space above the ground surface. In addition, building new and extending existing underground structure networks will become more important in order to upgrade city functions. Underground structures are usually connected to their adjacent structures for convenience. However, the underground structures connected to others are often owned by various organizations, designed with different codes, and/or constructed at different times. Hence, accurate assessment of seismic performance and prediction of behavior around the in-ground joints are significantly difficult in many cases. On the other hand, the in-ground joints of multiple underground structures with different seismic properties tend to induce relative seismic responses, localized stress, deformation and failure. Therefore, it is important to obtain a benchmark case history of the seismic behaviors around the joints.

In light of this, a research project on seismic behavior of underground structure joints was conducted. To capture the localized behavior around the joints, a large number of sensors need to be placed around the joints. However, it is quite difficult to do that in small-scale structure models because of their insufficient space for installation of many various sensors. Therefore, a series of shaking table tests with fully-instrumented large structure models was performed at the end of February 2012.

The shaking table used for this test is one of the world largest facilities, E-Defense at Hyogo Earthquake Engineering Research Center, National Research Institute for Earth Science and Disaster Prevention (NIED), Japan. The test specimen was composed of soil and large-scale structural models such as two vertical shafts interconnected with a cut-and-cover tunnel and two shield tunnels with sharply curved portions crossing a border of two different soil strata (Fig. 1). Because the model shafts and tunnels were 300- to 800-mm hollow circle or rectangle, there was a sufficient room in the models for installation of video cameras.

This paper provides a brief report of E-Defense test facilities, such as the E-Defense shaking table and soil container. In addition, fundamental information on the shaking table test including test setup, construction procedure, parts of test results, is introduced as an example of large model geotechnical engineering tests.

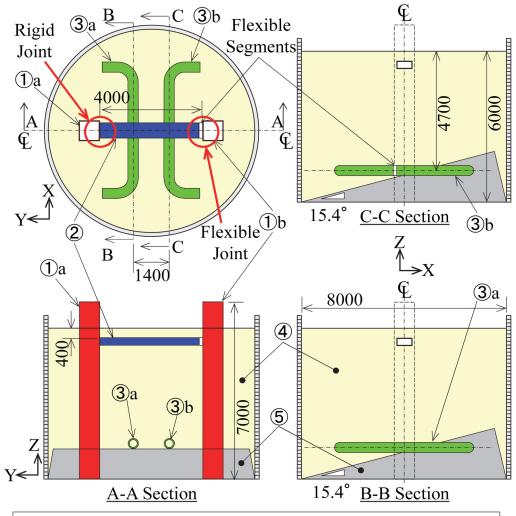

① Vertical Shafts, Aluminum, t = 12 mm, a: on rigid joint side, b: on flexible joint side
② Cut & Cover Tunnel, Aluminum, t = 8 mm
③ Shield Tunnels, Acrylic Plastic, t = 12 mm, a: w/o flexible segment, b: w/ flexible segment
④ Surface Layer, Wet Albany Silica Sand, w = 5%, Dr = 55%
⑤ Inclined Bedrock, Cement-mixed Soil, Vs = 350 to 400 m/s

Figure 1. Test Setup.

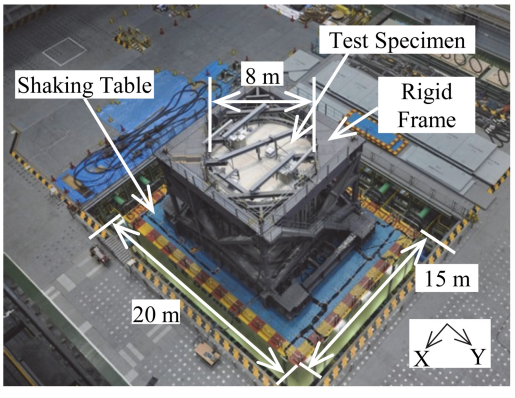

Figure 2. E-Defense Shaking Table.

2 ON E-DEFENSE FACILITIES

For geotechnical shaking table experiments on liquefaction, earth structures, soil-pile-structure and soil-underground structure interaction, a shaking table with sufficient capacity is very important. The capacity of the shaking table means the maximum acceleration, velocity and displacement as well as its dimensions and payload. In addition, a data acquisition system needs to have a sufficient number of channels and size of data recording memory. A soil container is usually necessary as well. In this chapter, E-Defense test facilities are briefly presented.

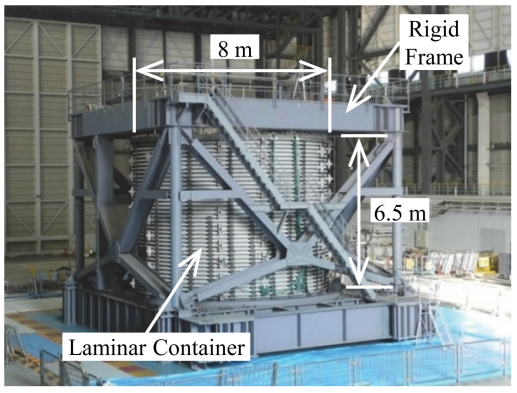

Figure 3. Laminar container.

2.1 *E-Defense shaking table*

In the 1995 Kobe Earthquake, a large number of buildings were damaged, and therefore, demands for more researches on seismic performance of buildings rapidly increased. In light of this, E-Defense was designed and built to excite full- or large-scale test specimens with real earthquake motions recorded in various areas in 1995. The size of the shaking table is 15 m by 20 m (Fig. 2) and its payload is 12 MN. More detailed performance of the E-Defense shaking table until the most recent update is available in Ohtani et al. (2003). In 2012 and 2013, the E-Defense shaking table was upgraded in order to capture detailed behavior of test specimens with more than 800 sensors as well as inputting long-duration motions recorded in the 2011 Tohoku Earthquake. Details of the upgraded performance will be available in near future.

2.2 *Laminar container*

There are two types of soil containers in E-Defense. One of them is a rectangular parallelepiped rigid container, and the other is a cylindrical laminar container. The section size and height of the former container are 16 m by 4 m and 5 m, respectively. This rigid container has been employed by experiments on plane strain tests, for instance, retaining walls and quay walls. The latter container is often used when large ground deformation is expected. Choice of the containers is highly dependent on purposes, structures of interest and expected behaviors. Because the laminar container was used in the present study more details are described herein.

The E-Defense laminar container is shown in Figure 3. Internal diameter and depth of the container are 8 m and 6.5 m, respectively. It is composed of 40 rings and linear sliders between the rings in order to minimize the friction. The sliders are a pair of single-dimensional linear sliders smoothly moving in the radial and circumferential directions. For smooth sliding, there is certain length of clearance between the sliders, and therefore, vertical motion of the rings is possible to some extent.

The rigid frame around the container in Figure 3 is also a very important element of the container. The frame is used as an access to the container top, working platform and jig for sensors because it is very rigid and its behaviors during shaking is identical to the shaking table without significant deflection.

In addition, two types of rubber sheets are placed between the container wall and the model ground. One of them is a sheet of rubber membrane installed next to soil, and the other is a sheet of lubrication rubber placed between the rubber membrane and the container wall. Roles of the former and the latter rubbers are prevention of water leakage and minimization of boundary effects from the container wall to the internal soil as well as protection of the rubber membrane.

3 ON TEST SPECIMEN

Using E-Defense, totally 5 large-scale shaking table experiments on soil-structure interactions have been performed until April, 2014. The E-Defense large-scale experiments performed in the past are summarized in Table 1. Four experiments were conducted in 2006 in Dai-Dai-Toku Project (Ministry of Education, Culture, Sports, Science and Technology and National Research Institute for Earth Science and Disaster Prevention 2006, 2007), and another series of experiments were carried out in 2012 (Kawamata et al. 2012, 2013). Introducing the latest experiment as an example, potential of E-Defense large-scale shaking table tests is described in this paper.

3.1 *Details of tested model ground*

Figure 1 showed the test setup of the specimen. The tested specimen was composed of 2 different soil strata and 5 underground structure models.

The soil strata were surface layer underlaid by inclined bedrock. The surface layer was made of wet sand, and its average water content and relative density were approximately 5% and 55%, respectively. The inclined bedrock was built by mixing cement and sand that was used for the surface layer. The shear wave velocity of the bedrock ranged from 350 to 400 m/s. The tested sand was #48 Albany Silica sand. The same sand was used for the previous series of experiments in 2006, and therefore, details of the soil characteristics are available in Ministry of Education, Culture, Sports, Science and Technology and National Research Institute for Earth Science and Disaster Prevention (2006, 2007). Because the soil material has been used several times, careful attention was to change of its characteristics due to washing of its fines content.

The large-scale underground structure models consisted of 2 vertical shafts interconnected with a cut-and-cover tunnel and 2 shield tunnels crossing the border between the inclined bedrock and the surface layer. The cross section shape and the size of the structure models are shown in Figure 4. All the models were of approximately 1/20 size and typical shapes

Table 1. Summary of E-Defense soil tests.

Year	Container used	Soil material used	Structure in interest
2006	Laminar	Dry sand	Pile foundation
	Rigid	Liquefiable sand	Sheet pile quay wall
	Laminar	Liquefiable sand	Pile foundation
	Rigid	Liquefiable sand	Caisson quay wall
2012	Laminar	Wet sand	Underground structures

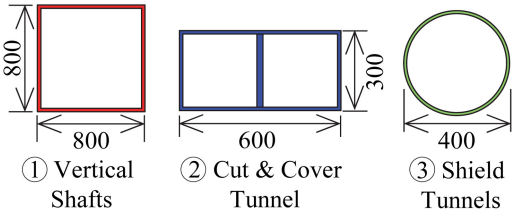

Figure 4. Section shape and dimensions of structure models.

of their prototype structures. Materials and wall thicknesses of the models were carefully selected to produce equivalent stiffness of their scaled-down prototypes.

The tunnel that was connected to the shafts examined the process of localized damage development around their joints as well as the dynamic behavior of the coupled underground structures. Flexible segment was placed at one of the joints, “flexible joint”. Moreover, the joint without is called “rigid joint” in this paper (refer to Fig. 1). Details of both joints are illustrated in Figure 5. The test specimen was shaken on 3 days, February 23, 24, and 28, 2012, and types of the joints were modified between the 2nd and the 3rd shaking days. In the first 2 days, stainless steel bolts were used in order to sufficiently fix the cut-and-cover tunnel to the vertical shaft at the rigid joint. On the other hand, the stainless steel bolts except ones in the bottom line were replaced by resin bolts to deliberately represent inappropriate joint. The flexible segment of the flexible joint was made of hollow rectangular rubber pieces alternately laminated with steel plates in order to prevent significant deformation by earth pressure from surrounding soil. The flexible segment was active in the first 2 days (Fig. 5b top), but was made inactive by fixing with bolts in order to concentrate damage at the decayed rigid joint on the 3rd day (Fig. 5b bottom). It is important to mention the ground surface was leveled by erasing cracks upon the above modification of the joint types between the 2nd and the 3rd days.

Moreover, the shield tunnels were tested to better understand the localized behaviors around the border between the rigid cement-mixed soil and the relatively

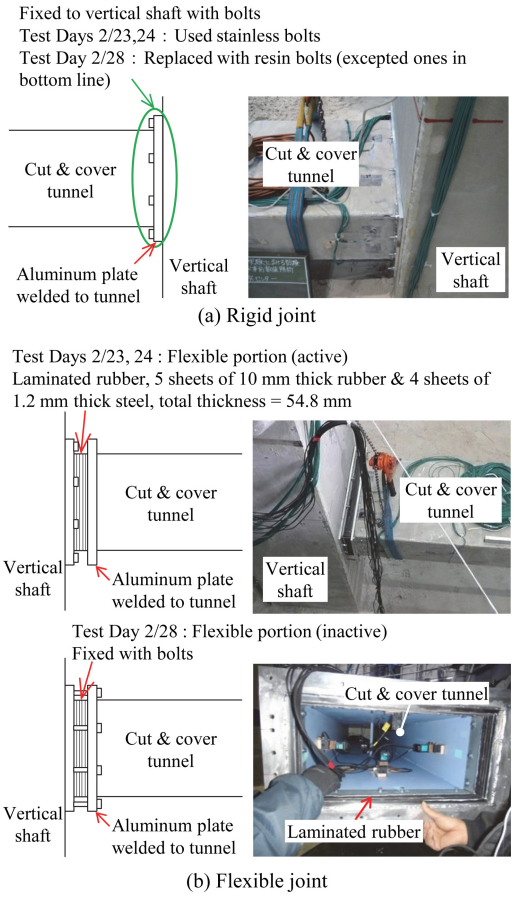

Figure 5. Details of joints.

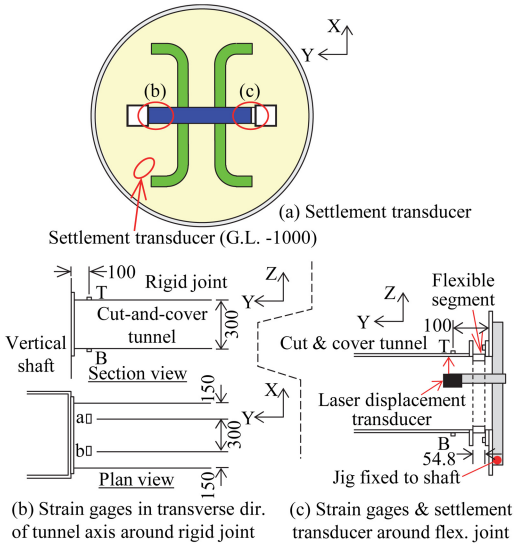

Figure 6. Locations of sensors at shallow depth.

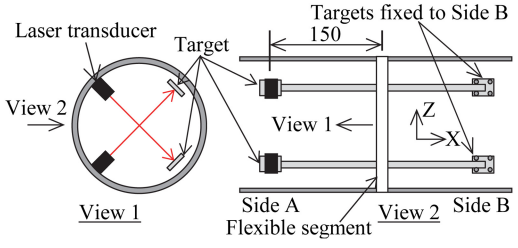

Figure 7. Displacement transducers at flexible segment along shield tunnel.

soft surface layer. In addition, one of the shield tunnels had a flexible segment right at the border of the different soil strata, and the other did not in order to examine the influence of the flexible segment.

Using almost full capacity of E-Defense data acquisition system, more than 800 various sensors, such as strain gauges, inclinometers, accelerometers, displacement and velocity transducers, were installed in/on the soil, along/in/on the structure models, on the container and the shaking table. Figures 6 and 7 present locations of ground settlement transducer, strain gages around the joints, displacement transducers at the flexible joint and in the shield tunnel. In addition, 3 tiny high-speed cameras with LED lights were installed at both the joints and around the flexible segment along the shield tunnel to observe behavior in the structure models (Fig. 8).

3.2 *Construction procedure of test specimen*

Considering the cost for research and construction as well as workers' safety, reasonable construction procedure had to be selected for model tests. Therefore, it is very important to summarize construction procedure of the test specimen also as reference for future experiments. Furthermore, assessment of the construction procedure probably helps make more engineering analyses on the test results. In this chapter, construction procedure of the tested specimen is briefly described.

First, the vertical shafts were placed in the empty container. Because these 2 shafts were interconnected with the cut-and-cover tunnel later, their setting locations were carefully surveyed, and then the shafts were fixed at their tops and the bottoms to the container in order to make no translation of the shafts during placement of the soil material (Fig. 9A).

Second, the cement-mixed sand and the wet sand layer were placed by compacting with vibro-plate from the bottom of the container (Fig. 9B) until the height of the soil strata reached the level of the shield tunnels. At the same time, sensors were installed in the ground. Thereinafter, two shield tunnels were carefully set at the precise location (Fig. 9C). After that, the soil material was placed on the tunnel models and compacted taking care not to damage the sensors, their cables, and the structure models.

Because of the time schedule of the E-Defense shaking table, the specimen was constructed not on the

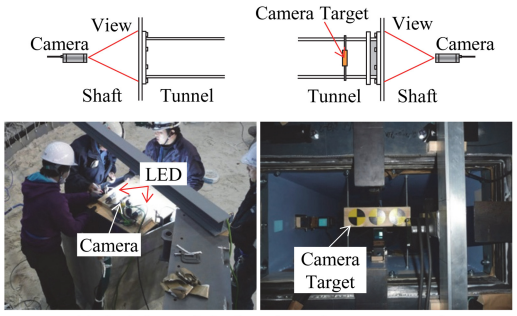

(a) At joints of shaft and cut & cover tunnel

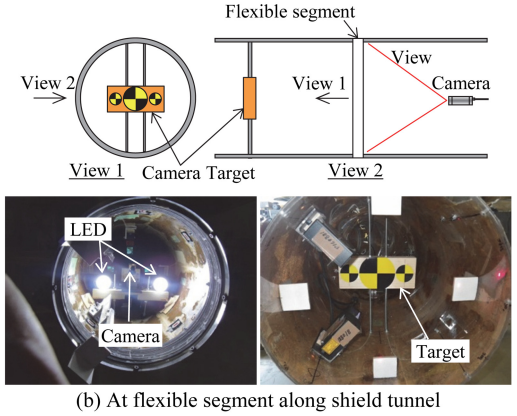

(b) At flexible segment along shield tunnel

Figure 8. Placement of tiny high-speed video camera.

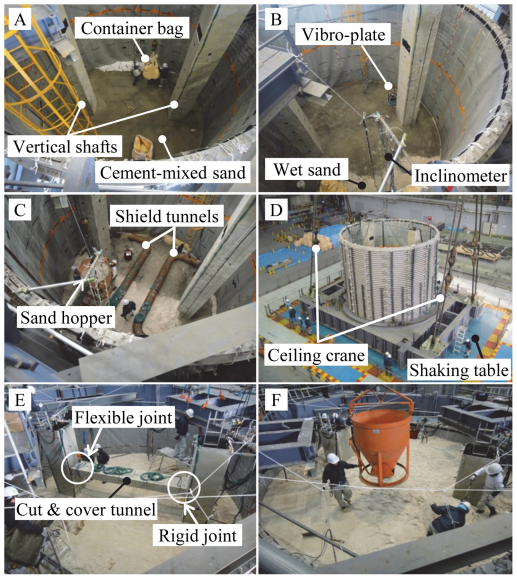

Figure 9. Construction procedures.

shaking table until this stage, and moved onto the shaking table. Placement of the model on the shaking table is shown in Figure 9D. When the height of the soil strata reached the level of the cut-and-cover tunnel, the tunnel was fixed to the shafts with and without the flexible segment (Fig. 9E). Because the flexible segment could not support the dead weight of the tunnel, the tunnel was temporarily hung up by a chain block at the flexible joint.

Finally, the rest of the surface layer was constructed (Fig. 9F) until the soil layer reached at 6 m from the bottom. After completion of the construction, high-speed video cameras, sensor fixers, sensors and targets for displacement transducers were placed. In addition, some ground investigations (i.e. measuring shear wave velocity with bender elements embedded in the test ground, Dutch cone penetration test, and surveying ground surface) were carried out in order to verify characteristics of the tested soil.

Table 2. List of input motions.

	Motion	Acc. Level[1)]	Direction[2)]
1st Day 02/23	Step Sine	0.1 m/s^2	0 Deg.
	1–20 Hz	0.1 m/s^2	90 Deg.
		0.3 m/s^2	0 Deg.
		0.3 m/s^2	90 Deg.
		0.3 m/s^2	30 Deg.
		0.3 m/s^2	45 Deg.
		0.3 m/s^2	135 Deg.
2nd Day 02/24	Step Sine	0.3 m/s^2	90 Deg.
	1–20 Hz	0.5 m/s^2	0 Deg.
		0.5 m/s^2	90 Deg.
	Takatori	50%	See Note[3)]
3rd Day 02/28	Step Sine	0.3 m/s^2	90 Deg.
	1–20 Hz	0.3 m/s^2	0 Deg.
	Takatori	80%	See Note[3)]

1) "Acc. level" shows the maximum acceleration for Step Sine motions, and amplification from the actual records for Takatori motion.
2) "Direction" means angle from x-axis; i.e. 0 degree is x-axis and 90 degree is y-axis.
3) EW and NS components of Takatori were put in x- and y-axes, respectively.

3.3 *Input motions*

Table 2 shows the summary of motions applied to the test specimen. 2 types of motions were used in this test series.

First, Step Sine waves with various amplitudes were used as the basic input motion to obtain fundamental test data. The Step Sine motion is a sequence of 2-cycle component signals whose frequency increased stepwise from 1 to 20 Hz. For better hydraulic control, 4-second tapering motions were added before and after the main part of Step Sines. Because of geometry of the test specimen, anisotropic behaviors were expected, and therefore, the Step Sine motions were put in various directions. More details are available elsewhere (Kawamata et al. 2012).

Takatori motion recorded in 1995 Kobe Earthquake (Nakamura et al. 1996) was one of the most typical motions for experimental input motions because it can cause large ground displacement. Assuming the axial

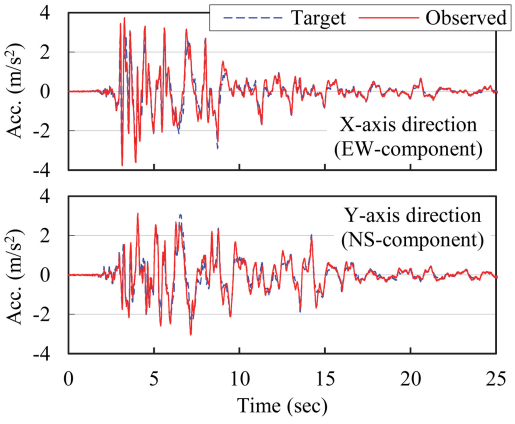

Figure 10. Time histories of table motions (Takatori 50%).

direction of the cut-and-cover tunnel (Y-axis in Fig. 1) was the most critical direction, the main component of the Takatori motion, its North-South component, was put in Y-axis, and East-West component was in X-axis (refer to Fig. 1). Because the test specimen is relatively complicated, no vertical motion was applied in order to eliminate its influence.

A comparison of the target motion and the real table motion in Takatori 50% shaking is shown in Figure 10. Sometimes, target and table motions are different because of interactions between actuators, shaking table and test specimen, but both the motions in Figure 10 are in good agreement. The same tendency appeared also in Takatori 80% shaking.

4 EXAMPLE TEST RESULTS

In this series of shaking table experiments, a large number of useful data including sensor records, movies, inspection and surveying results, were obtained. In this chapter, some test results are introduced as examples. More test data are available in Kawamata et al. (2012, 2013) and will be further published in near future.

4.1 *Failure of joint during strong shaking*

Failure of the flexible and the rigid joints occurred during Takatori 50% and 80% shaking, respectively. Sequence of the failure can be tracked in detail by movies taken by high-speed cameras.

Figure 11 shows failure sequence of the flexible joint in Takatori 50%. Glue bonding a rubber and a steel plate of the laminated flexible segment may be insufficient, and therefore, it started detaching during strong motion (Figs 11B, C). This detachment induced significant settlement of the tunnel around the flexible joint (Fig. 11D).

Failure sequence of the rigid joint recorded in Takatori 80% is presented in Figure 12. In the first couple of significant peaks of Takatori motion, heads

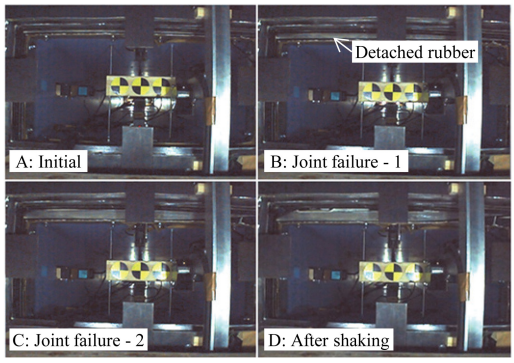

Figure 11. Failure of flexible joint in Takatori 50%.

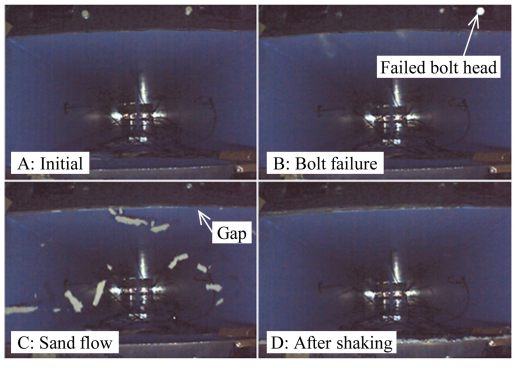

Figure 12. Failure of rigid joint in Takatori 80%.

of the most resin bolts were popped away (Fig. 12B). After that, the gap at the top of the failed joint alternately opened and closed during shaking. Only when width of the gap became significantly large, soil around the failed joint flowed into the tunnel (Fig. 12C). After shaking, the sand flow did not continue even though the gap still opened (Fig. 12D).

4.2 *Sectional deformation during strong motion*

Figure 13 shows the sequence of sectional deformation of the shield tunnel. The photos in this figure were taken by a tiny high-speed camera placed in the hollow space inside the shield tunnel with a flexible segment (Fig. 8b). Condition of the shield tunnel before excitation of Takatori 80% motion is shown in Figure 13A. The steel rods supporting the camera target were initially straight, but deformed during the previous excitation, especially in Takatori 50% motion. Figures 13B, C show sectional deformation during shaking. Arrows in the figures show deformation directions at that time. In these figures, the section of the shield tunnel obviously deformed to a rugbyball-shape. Also, it is noticeable that a sensor target (white rectangular plate at the top center of Fig. 13) at the top of the tunnel appeared more in Figure 13D than Figure 13A. It implies that the sectional deformation of the tunnel is combination of rugbyball-shaped

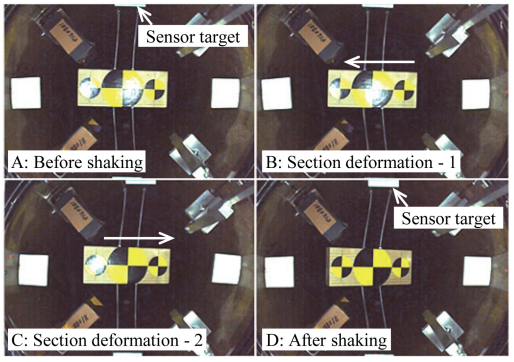

Figure 13. Section deformation around flexible segment along shield tunnel in Takatori 80%.

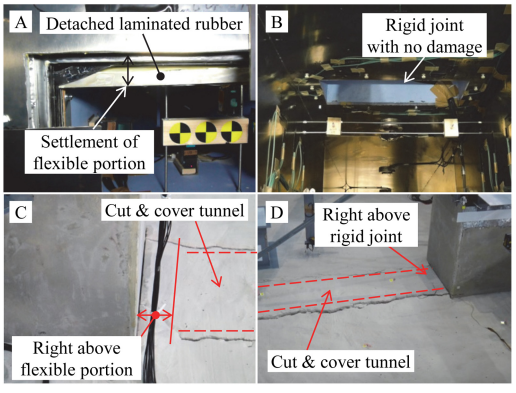

Figure 14. Inspection results after Takatori 50%.

deformation and crushed deformation in the vertical direction.

4.3 *Results of inspection*

The tested model was inspected in order to find useful information to help understanding what happened with the test specimen during shaking. After excitation with Takatori 50% on the 2nd test day, the ground surface and shallow portion of the ground around the cut-and-cover tunnel were investigated. In addition, the entire test specimen was inspected at dismantlement of the specimen after completion of all the shaking.

Results after Takatori 50% are summarized in Figure 14. Figure 14A shows significant settlement of the flexible segment due to detachment between a rubber piece and a steel plate, and corresponds to Figure 11D. The settlement reached more than 20 mm. On the contrary, no damage was observed at the rigid joint as shown in Figure 14B. Significant cracks on the ground surface are shown in Figures 14C and D. The cracks run along the cut-and-cover tunnel. This phenomenon indicates that the ground right above the tunnel showed less settlement than in the other area because the tunnel was supported by the vertical shafts, and then, this difference of the settlement induced the cracks.

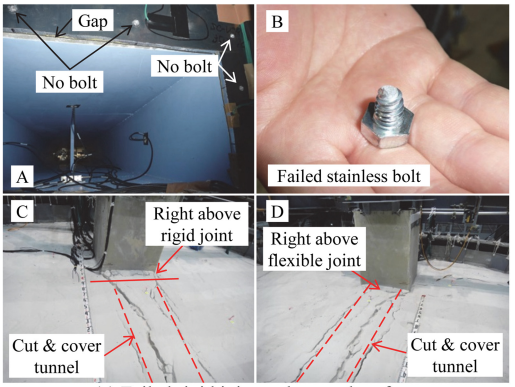

(a) Failed rigid joint and ground surface

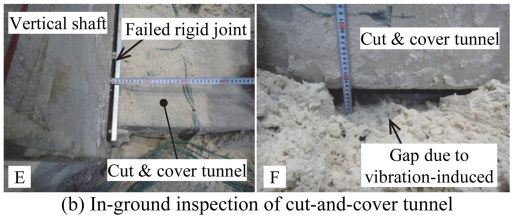

(b) In-ground inspection of cut-and-cover tunnel

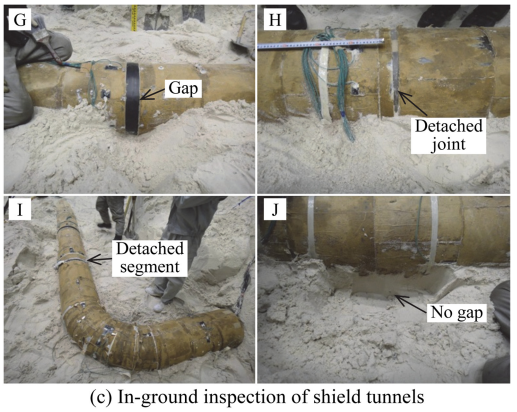

(c) In-ground inspection of shield tunnels

Figure 15. Inspection results after Takatori 80%.

Figure 15 presents inspection results after Takatori 80% shaking. The failed rigid joint is shown in Figure 15A. Except 2 stainless steel bolts in the bottom line, all the bolts completely failed. Figure 15B shows one of the failed stainless steel bolt heads. Cracks on the ground surface are shown in Figures 15C, D. It is noticeable that only 2 cracks were observed at the end of the 2nd day testing, but several significant cracks appeared after Takatori 80% shaking.

Figure 15E shows the gap at the failed joint. Width of the gap was approximately 15 mm at maximum. Approximately 70-mm-deep gap was observed beneath the cut-and-cover tunnel (Fig. 15F). It is consistent with mechanism of crack generation on the ground surface mentioned above and probably it significantly affected the behavior of the vertical shafts as well as the cut-and-cover tunnel.

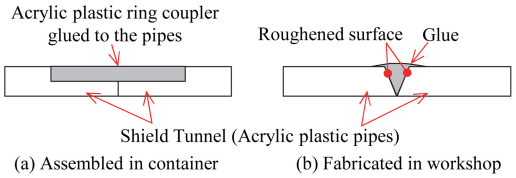

Figure 16. Joints along shield tunnel.

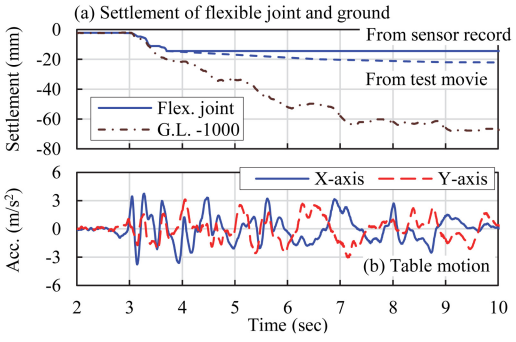

Figure 17. Comparison of settlement of flexible joint and ground, and input motion in Takatori 50%.

Figures 15G–J present inspection results of the shield tunnel. Minor gap was observed around the flexible segment (a black band at the center in Fig. 15G). Because the shield tunnels were built by connecting 1 m long acrylic plastic pipes in 2 different ways (Fig. 16), there were some joints along the tunnels, and some of the joints illustrated in Figures 16a, b were detached as shown in Figures 15H, I, respectively. In Figure 15J, no gap beneath the tunnels was observed.

4.4 *Mechanism of joint failure in large motions*

Time histories of displacement at the flexible segment and ground settlement at G.L. −1.0 m are compared in Figure 17a. Both data were directly measured by displacement transducers. For references, settlement of the flexible joint assessed by the movie and the table motion are plotted together. The measured displacement of the flexible segment reached the maximum at approximately 18 mm because the settlement exceeded the capacity of the transducer. In this figure, it is obvious that the settlement of the flexible segment is highly correlated with the ground settlement because both the settlement started at the beginning of the significant motion in Takatori shaking (refer to Fig. 17b) and gradually increased together.

Figure 18 shows time histories of axial strains along the cut-and-cover tunnel around the failed joint and ground settlement at G.L. −1.0 m in Takatori 80%. Also, table motion is plotted as reference. In Figure 18a, significant strain jump appears about at 3.3 second. According to the test movie, this jump probably corresponds to the failure of the resin bolts because it occurred in the first couple peaks of accelerations in Takatori motion (refer to Fig. 18c). On

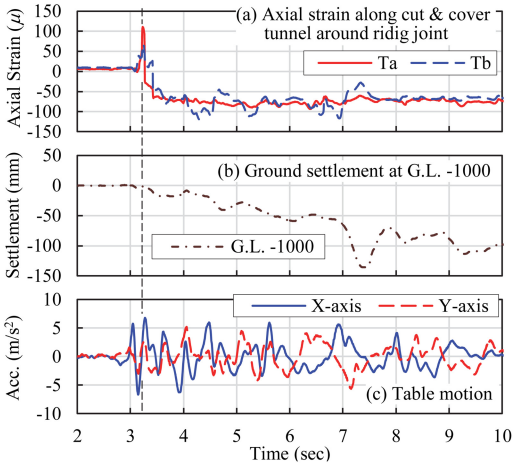

Figure 18. Comparison of axial strain cut & cover tunnel around rigid joint, ground settlement, and input motion in Takatori 80%.

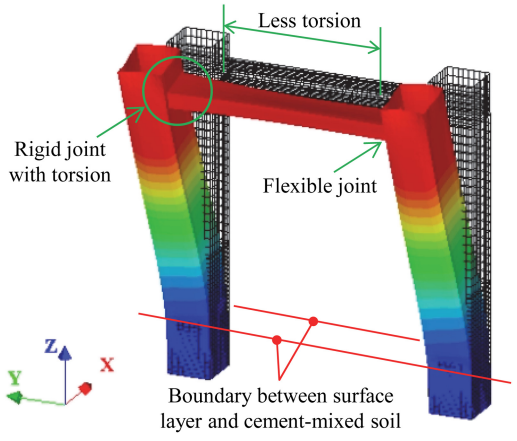

Figure 19. Torsion of cut & cover tunnel in 3D numerical analysis at 3.39 second in Takatori 50%.

the other hand, the time history of the soil settlement at G.L. −1.0 m shows no significant change at this time (Fig. 18b). Comparing these data, it is reasonably concluded that insufficient seismic resistance of the rigid joint resulted in the failure.

4.5 *Soil-structure-structure interactions*

After completion of the series of shaking table tests, 3-dimensional numerical analysis was conducted with solid and shell elements. Figure 19 shows the deformed shape magnified 100 times at 3.39 second during Takatori 50% motion. The most noticeable observation of this figure is torsion of the cut-and-cover tunnel around the rigid joint. This torsion becomes less significant as distance from the rigid joint increases, and finally it becomes very small near the flexible joint.

Some examples of strain time histories in transverse direction of the tunnel axis recorded in the shaking

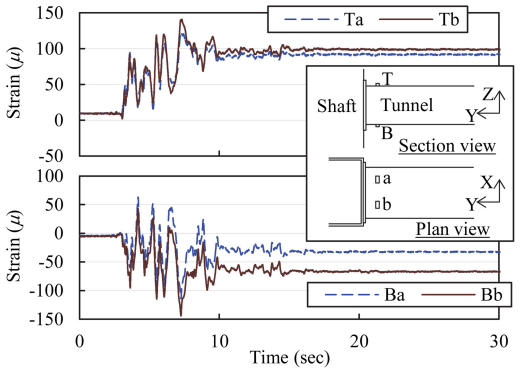

Figure 20. Time histories of transverse strain along cut & cover tunnel around rigid joint in Takatori 50%.

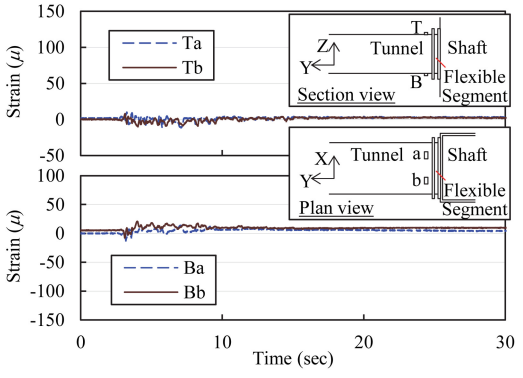

Figure 21. Time histories of transverse strain along cut & cover tunnel around flexible joint in Takatori 50%.

table tests are plotted in Figures 20 and 21 in order to find influences of its torsional behavior. Comparing these figures, it is quite apparent that the strain in transverse direction of the tunnel axis around the rigid joint is much larger than around the flexible joint. It implies that only the flexible segment deformed and minor deformation of the tunnel occurred around the flexible joint. It seems consistent with Figure 19. From Figure 20, the top of the tunnel was stretched and the bottom was compressed near the rigid joint.

A free body diagram with possible forces acting around the rigid joint is illustrated in Figure 22. When the shaft rotates due to its deflection, the cut-and-cover tunnel also rotates with the shaft. However, overburden stress from the ground above the tunnel worked as resistant force against the rotation. Because of this rotational resistance, the top of the tunnel intends to be stretched in the transverse direction, and probably the bottom will be compressed at the same time. This tendency is exactly shown in Figure 20. At a sufficient distance from the joint, the rotation of the tunnel becomes minor, and therefore, the torsional deformation is induced only near the joint. It is important to note that the vibration-induced gap beneath the tunnel (refer to Fig. 15F) probably provided significant

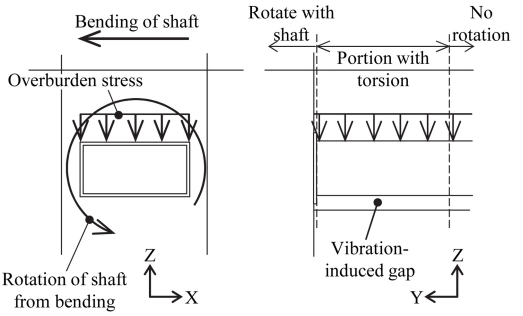

Figure 22. Free body diagram around rigid joint.

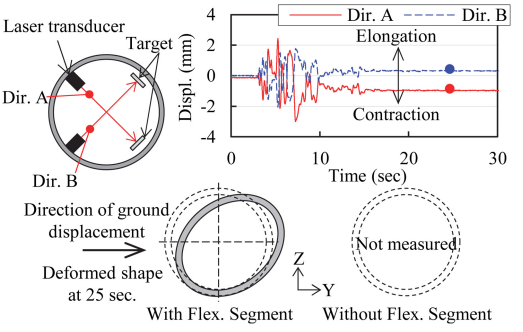

Figure 23. Displacement of shield tunnel in diagonal direction in Takatori 50%.

contribution to the dynamic behaviors of the tunnel as well as failure mechanism around the joint. For reasonable engineering assessment of this torsional deformation along the tunnel, more analyses on the test results are necessary.

4.6 *Section deformation of shield tunnel*

Time histories of diagonal displacement of the shield tunnel with the flexible segment (refer to Figs 1, 7) are shown in Figure 23. In this figure, it is apparent that the displacements in direction A and B are out-of-phase. Because the laser transducers and targets were connected to the opposite sides of the tunnel across a flexible joint, the recorded displacement is a combination of the deformation of the tunnel cross section and the lateral deformation at the flexible joint. However, this tendency is consistent with observations shown in Figure 13; i.e. the section of the shield tunnel deformed from circle-shaped to rugbyball-shaped. Direction of the deformation is also illustrated in Figure 23, and probably highly depends on direction of the ground displacement. This sectional deformation is probably affected by the flexible segment, but unfortunately it was not measured along the tunnel without the flexible segment in this series of experiments. More numerical researches as well as more analyses on the obtained test results are expected.

5 CONCLUSIONS

Using the world largest E-Defense shaking table, the series of the shaking table tests on dynamic behavior of soil-underground structure interaction was performed to obtain better understanding. The following conclusions were drawn:

(1) Large-scale shaking table tests have great advantages to obtain important information about localized behaviors and capture phenomenon with video cameras.
(2) Flexible and rigid joints indicated different failure modes. The former showed significant settlement at flexible segment, but the latter failed due to lack of its seismic performance.
(3) Localized behaviors appeared around rigid in-ground structural joints. These special behaviors probably occur in multiple underground structures connecting each other and surrounding soil, but not in single underground structure and soil. These localized behaviors cannot be captured in 2-dimensional numerical models traditionally used in design practice. Establishment of effective 3-dimensional numerical models is one of the important future research topics.
(4) Significant deformation was observed even along the shield tunnel with flexible segment. It implies that more significant deformation happened in the tunnel without the flexible segment. More research is required for improved evaluation of dynamic behavior of underground structures.

AKCNOWLEDGEMENT

For great succession of this research project, many advice and opinions were provided by Professor Maekawa (University of Tokyo), Dr. Hosoi (TUG's Corp.) and Dr. Goto (University of Tokyo). In addition, Dr. Tabata and Dr. Kajiwara (National Research Institute for Earth Science and Disaster Prevention) helped for initial planning of this research. All their supports are greatly acknowledged.

REFERENCES

Kawamata, Y., Nakayama, M., Towhata, I., Yasuda, S. & Tabata, K. 2012. Large-scale Experiment using E-Defense on Dynamic Behaviors of Underground Structures during Strong Ground Motions in Urban Areas, 15th World Conference of Earthquake Engineering, Lisbon.

Kawamata, Y., Nakayama, M., Towhata, I., Yasuda, S., Maekawa, K. & Tabata, K. 2013. Considerations on Seismic Behaviors of In-ground Structural Joint observed in E-Defense Large-scale Experiment, 6th Civil Engineering Conference in Asia Region, Jakarta.

Ministry of Education, Culture, Sports, Science and Technology and National Research Institute for Earth Science and Disaster Prevention. 2006 Research Theme No. 2 Annual Report of the fiscal year 2005, Special project for earthquake disaster mitigation in urban areas (in Japanese).

Ministry of Education, Culture, Sports, Science and Technology and National Research Institute for Earth Science and Disaster Prevention. 2007. Research Theme No. 2 Annual Report of the fiscal year 2006, Special project for earthquake disaster mitigation in urban areas (in Japanese).

Nakamura, Y., Uehan, F. & Inoue, H. 1996. Waveform and its Analysis of the 1995 Hyogo-Ken-Nanbu Earthquake (II), JR Earthquake Information No. 23d.

Ohtani, K., Ogawa, N., Katayama, T. and Shibata, H. 2003. Construction of E-Defense (3-D full-scale earthquake testing facility), 2nd International Symposium on New Technologies for Urban Safety of Mega Cities in Asia, pp. 69–76.